Improving Irrigation Scheduling through Deep Learning-Based Reference Evapotranspiration Estimation

Praveen Kumar Khandappa
Department of Computer Science and Engineering, University of Visvesvaraya College of Engineering, Bangalore University, Bengaluru, India
pksjp2013@gmail.com (corresponding author)

Manjula Sunkudkatte Haladappa
Department of Computer Science and Engineering, University of Visvesvaraya College of Engineering, Bangalore University, Bengaluru, India
shmanjula@gmail.com

Received: 22 September 2025 | Revised: 9 October 2025 | Accepted: 15 October 2025

 DOI: https://doi.org/10.48084/etasr.15002

ABSTRACT

Agricultural water management is one challenging issue for farmers. The estimation of accurate crop watering plays a vital role in improving yield and water management. Reference Evapotranspiration (ET0) is a weather-based parameter that can help estimate crop water requirements. This study investigated Artificial Neural Network (ANN), Convolutional Neural Network (CNN), and Long Short-Term Memory (LSTM) models for ET_0 prediction. The proposed ANN model achieved a Mean Squared Error (MSE) of 0.1246 and an R-squared (R^2) of 0.9588. The CNN model was limited by the lack of spatial patterns, and the LSTM did not perform as well as it could due to minimal sequential dependencies. The results of this study show the importance of aligning model architecture with dataset characteristics.

Keywords-agricultural water management; reference evapotranspiration (ET_0); Artificial Neural Network (ANN); Convolutional Neural Network (CNN); Long Short-Term Memory (LSTM); crop water requirement prediction

I. INTRODUCTION

Water is an essential input for agriculture, and farmers struggle to manage it effectively, especially in regions vulnerable to climatic variability. In examining the estimation of crop water requirements, irrigation scheduling, and water use efficiency, the proper estimation of the reference Evapotranspiration (ET_0) is crucial [1]. ET_0 is the term used to describe the atmospheric demand for water and is also used as a reference to compute crop evapotranspiration, which is the foundational element of irrigation scheduling and climate-related crop studies. The ET_0 has traditionally been estimated with the FAO-56 Penman-Monteith equation. This formula considers various meteorological conditions, such as temperature, humidity, solar radiation, and wind speed [2]. Although this method is physically robust, it requires a large amount of high-quality meteorological information that is often poor or not available for many agricultural regions. In recent years, there has been a shift toward data-driven methods to avoid the restrictions that are associated with conventional techniques. Within this data-driven landscape, different model architectures exploit different inductive biases.

In the case of tabular meteorological inputs, feed-forward Artificial Neural Networks (ANNs) are highly efficient universal approximators. Convolutional Neural Networks (CNNs) perform exceptionally well when the spatial structure is informative. Sequential models, especially Long Short-Term Memory (LSTM) networks, can capture temporal dependences in weather time series [3]. The alignment of design with data characteristics (that is, geographical, temporal, or mixed) and the adoption of hybrid pipelines that combine weather-station and remote-sensing data are becoming increasingly important in comparative research. The modeling of complicated non-linear interactions between weather factors and ET_0 has been made possible by recent developments in Machine Learning (ML) and Deep Learning (DL), which have opened the door to prospects for accuracy and efficiency improvements [4]. ANNs have been widely used because of their ability to capture nonlinear relationships in meteorological data sets. CNNs, initially developed for spatial data, have also been used to detect spatial hierarchies and patterns for climatic variables in the hydrological and remote sensing domains.

Recent advances in DL for geospatial and climatic modeling have expanded beyond conventional CNN and

LSTM architectures [5]. For instance, feature extraction and classification frameworks leveraging transfer learning and hybrid CNN structures have demonstrated strong performance in environmental prediction tasks. Effectively modeling the long-term dependency in time-series weather data, LSTM networks have been shown to achieve competitive performances in ET_0 forecasts. Similarly, transformer-based architectures have gained traction for remote-sensing-driven climatic forecasting, achieving enhanced spatiotemporal representation learning and robust generalization. Recent research has increasingly emphasized the role of data-driven models for accurate reference evapotranspiration (ET_0) estimation. In [6], several ML approaches were tested under limited meteorological inputs, finding that ensemble-based models consistently achieved lower Mean Squared Error (MSE) and higher coefficient of determination (R^2) than empirical baselines, highlighting the importance of careful feature selection. In [7], a systematic review of more than 300 papers found that ensemble learning models consistently achieve high stability, with typical R^2 values greater than 0.95 and RMSE between 0.1 and 0.6 mm/day, while the DL approaches perform well even with reduced inputs, such as only temperature data. In [8], an HS-LSTM variant was applied for daily ET_0 forecasting, achieving R^2 improvements of more than 0.05 compared to conventional LSTM, confirming the ability of hierarchical memory structures to capture short-term dependencies. In [9], a hybrid DL framework used feature reduction (PCA) to improve the accuracy of daily ET_0 prediction. In [10], CNN, GRU, and LSTM models were evaluated using meteorological data from Bangladesh, concluding that GRU and LSTM outperformed CNN (R^2>0.90), while the latter underperformed due to the absence of explicit spatial features.

In [11], remote sensing and meteorological factors were combined to reduce ET_0 prediction errors by up to 15% compared to models trained on meteorological-only datasets. In [12], the robustness of ANN pipelines was validated for daily ET_0 forecasting, reporting R^2 values consistently above 0.96 and superior accuracy compared to traditional regression techniques. In [13], hybrid DL strategies integrated solar radiation and RS variables, reducing MSE by nearly 10% relative to individual models. Expanding on architectural innovations, Temporal Convolutional Networks (TCN), LSTM, and N-BEATS were compared for ET_0 prediction in [14], finding that TCN achieved superior performance (R^2 > 0.94) with reduced error under limited-variable scenarios. In [15], hybrid empirical-ML frameworks were tested in semi-arid climates, reporting balanced results with R^2 above 0.92 and reduced overfitting risks, even when datasets were incomplete.

Previous works employing CNN, LSTM, and hybrid architectures largely focused on datasets with explicit spatial or temporal dependencies derived from remote-sensing or time-series inputs. In contrast, this study benchmarks standard DL models, ANN, CNN, and LSTM, on a non-temporal and non-spatial meteorological dataset, addressing an underexplored yet practically relevant scenario for ET_0 estimation. This comparative framing clarifies how the proposed work diverges from prior research by analyzing model suitability based on data structure rather than solely architectural complexity.

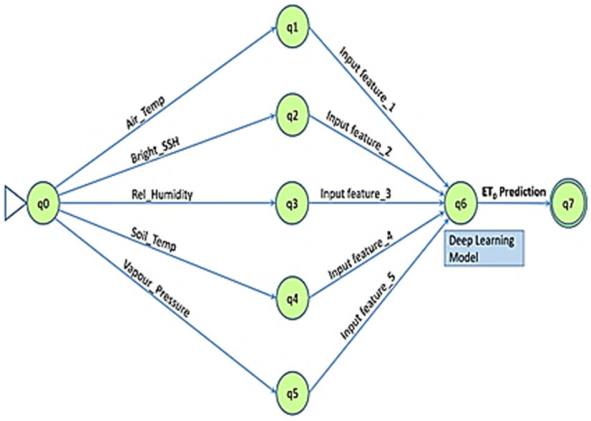

Fig. 1. Architecture for ET_0 prediction

II. PROPOSED METHODOLOGY

The study used meteorological data obtained from the University of Agricultural Sciences (UAS), Dharwad, India, located at 15° 30' 15.2" N latitude and 74° 15' 06.1" E longitude, with an elevation of approximately 683 m above sea level. The meteorological station at UAS Dharwad provides daily observations, and data spanning the years 2009 to 2020 were utilized in this work [16]. To ensure reliable performance evaluation, the dataset was divided into training (70%) and testing (30%) subsets. Figure 1 depicts the overall workflow of this study. Selected input variables were minimum and maximum air temperature (°C), bright sunshine hours (h), relative humidity (%), soil temperature (°C), and vapor pressure (kPa). All these parameters are crucial in controlling the atmospheric requirements of water and can therefore be considered as a relevant factor to estimate ET_0 [17].

After preprocessing and cleaning, 4,015 daily samples were used for model development. Outliers were filtered using the Inter-Quartile Range (IQR) method, and missing values (<2%) were estimated through linear interpolation to maintain temporal consistency. All variables were normalized to the [0, 1] range before training to ensure numerical stability and faster convergence.

The standard FAO-56 Penman Monteith equation was used to calculate the response variable ET_0. This model has been widely recognized as the most accurate for the estimation of reference evapotranspiration, as described in (1) [18].

$$ET_0 = \frac{0.408\,\Delta\,(Rn - G) + \gamma\,\frac{900}{(T+273)}u_2(e_s - e_a)}{\Delta + \gamma\,(1 + 0.34\,u2)} \quad (1)$$

where Rn is the net radiation at the crop surface (MJ per m^2 per day), G is the heat flux density in the soil (in MJ per m^2 per day), T is the average daily air temperature (°C), u_2 is the wind speed at a 2 m height (m/s), and e_s and e_a denote the saturation pressure and the actual vapor pressure (kPa), respectively. For the influence of atmospheric conditions on evapotranspiration, the slope of the vapor pressure curve ($\Delta, kPa \times C^{-1}$) and psychrometric constant ($\gamma, kPa \times C^{-1}$) were selected [19]. The ET_0 values estimated were used for training and testing the DL models, enabling an unbiased assessment against a baseline provided by prior research.

A. Deep Learning (DL) Architectures

The ANN, CNN, and LSTM are three commonly used DL architectures. In this study, to predict ET_0, three models were developed and compared with each other. The ANN was implemented as a fully connected feed-forward model, consisting of an input layer of 64 neurons (representing the embedded climatic features), a hidden layer activated by the ReLU function, and a single output neuron for regression. Each DL model was implemented in Python using TensorFlow and trained under identical configurations to ensure fair comparison. All models were trained for 200 epochs using the Adam optimizer with a learning rate of 0.01 and batch sizes of 8 and 100. A dropout rate of 0.2 was used to mitigate overfitting, while normal weight initialization was adopted to stabilize gradient updates. Early stopping (patience = 15 epochs) was applied to prevent overtraining. These hyperparameter choices were empirically tuned for optimal performance. The ANN was selected due to its demonstrated ability to learn complex non-linear structures in table data. This makes it well-suited for meteorological multitemporal data inputs, which are characterized by complex relations but have no clear spatial or temporal trend. The CNN architecture contained a 1D convolutional layer with 32 filters to capture the local patterns of input variables. A dense layer followed, with ReLU activation, and a flattening layer. Table I details the architectures of the models used.

TABLE I. SUMMARY OF DL ARCHITECTURES

Model	Architecture details	Optimizer and learning rate	Loss function	Batch size
ANN	Input: 64 neurons; Hidden: 1 layer (ReLU); Output: 1 neuron (regression)	Adam (0.01)	MSE	8, 100
CNN	1D Conv layer (32 filters) → Flatten → Dense (ReLU) → Output (1 neuron)	Adam (0.01)	MSE	8, 100
LSTM	LSTM layer (50 units, ReLU) → Output (1 neuron)	Adam (0.01)	MSE	8, 100

B. Training and Evaluation

All models were trained to maximize the regression accuracy. In view of the capabilities and performance of Adam to handle big data and its flexible learning rate setup, this optimizer is an excellent choice for DL-oriented applications. As shown in (2), MSE was used as the primary loss function to minimize the prediction errors during training [20].

$$MSE = \frac{1}{n}\sum_{i=1}^{n}(y_i - \hat{y}_i)2 \quad (2)$$

where y_i is the estimated ET_0, $\hat{y}_i$ is the observed ET_0, and n is the number of trials. A lower MSE means the closer the model predicts the actual values.

The model's efficiency was further assessed by calculating the coefficient of determination (R^2), an indicator of the proportion of the variance in the observed estimates that can be accounted for by the model itself [21], defined as:

$$R^2 = 1 - \frac{\sum_{i=1}^{n}(y_i - \hat{y}_i)2}{\sum_{i=1}^{n}(y_i - \bar{y}_i)2} \quad (3)$$

where $\bar{y}_i$ is the mean of the observed ET_0 values. An R^2 value close to 1 indicates high predictive power and better fitting of expected to actual values [22].

In addition to the above-mentioned statistical tests, for each model, scatter plots between predicted and observed ET_0 values were also constructed. These visualizations also yielded intuitive results for model alignment, revealing discrepancies and overall prediction scoring.

III. RESULTS AND DISCUSSION

The experiments on ANN, CNN, and LSTM offered very important hints that the architecture should match different data distributions. The results are presented according to forecasting accuracy, error indices, and visualization with scatter plots plotting forecasted against observed ET_0 values. Figures 2-4 illustrate the relationships between actual and predicted ET_0 values for the ANN, CNN, and LSTM models, respectively. Each scatter plot includes a regression line, an equation, and R^2 for visual clarity. The plots were generated using Matplotlib at 300 dpi resolution, with standardized font sizes (≥ 14 pt) and enhanced color contrast for improved readability.

A. Artificial Neural Network (ANN)

The ANN model performed better than the others in all evaluation criteria, with an MSE of 0.1246 and an R^2 of 0.9588. The scatter plot in Figure 2 reveals a good correlation between the predicted and measured values, since the points are closely packed around the 1:1 diagonal. The dense-connection structure of the ANN allowed it to capture fine-grained non-linear feature interactions, without explicit dependence on any spatial or sequential locality. Its versatility for extracting knowledge is particularly well-suited for atmospheric datasets in tabular form, where no explicit temporal or spatial hierarchies exist. Thus, ANN emerged as the most effective model in this study.

B. Convolutional Neural Network (CNN)

The CNN model achieved an R^2 of 0.9529 and an MSE of 0.1426, exhibiting marginally lower accuracy than the ANN while still showing strong predictive capabilities. The scatter plot in Figure 3 shows a good correspondence between predictions and actual values, albeit with slightly higher variance from the diagonal line. CNNs are inherently designed to extract local spatial patterns, but the model demonstrated its ability to infer hierarchical relationships between features, suggesting that CNNs may be considered when data contain latent or engineered spatial groupings.

C. Long Short-Term Memory (LSTM)

The LSTM model was the least effective among the three, with an R^2 value of 0.8890 and a relatively high MSE of 0.3361. The scatter plot in Figure 4 shows greater dispersion around the diagonal, reflecting weaker predictive alignment with observed ET_0 values. LSTMs are optimized for datasets with sequential or temporal dependencies; however, the absence of inherent temporal signals in the dataset restricted the utility of memory cells and gating mechanisms, leading to underutilization of the LSTM architecture and poorer generalization.

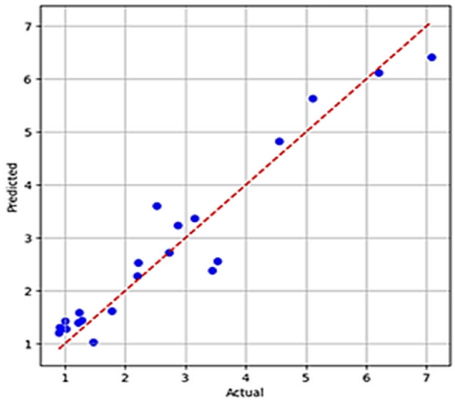

Fig. 2. Scatter plot of ANN model predictions versus observed values.

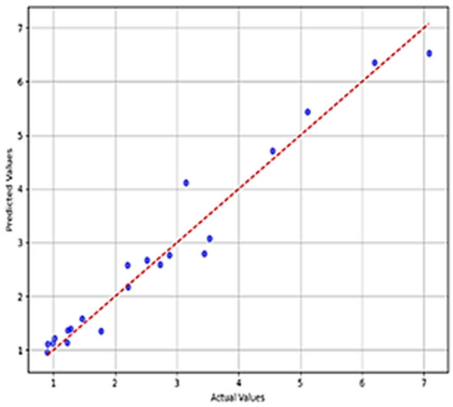

Fig. 3. Scatter plot of CNN model predictions versus observed values.

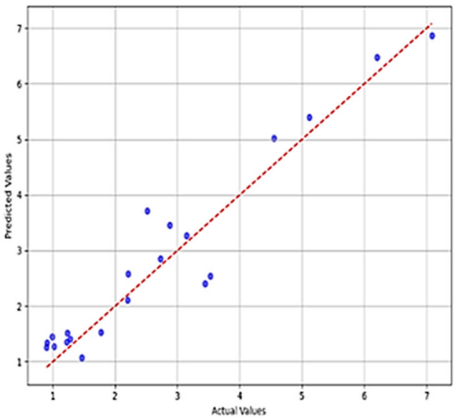

Fig. 4. Scatter plot of LSTM model predictions versus observed values.

D. Comparative Performance

Table II presents a summary of the three models' performance. The ANN model demonstrated the best predictive accuracy and error minimization, while the CNN provided competitive results with marginally lower performance. In contrast, LSTM's sequential learning capacity was not advantageous for the static dataset used in this study. These findings emphasize that model selection should be data-centered, prioritizing compatibility with intrinsic data properties rather than architectural complexity.

The fully connected structure of the ANN was optimal for capturing non-linear interactions in this dataset. The reliance of CNN on spatial features limited its effectiveness in the absence of explicit spatial patterns, while LSTM's sequential modeling capability was underutilized in the absence of temporal dependencies.

TABLE II. PERFORMANCE OF THE THREE MODELS

Model	MSE	RMSE	MAE	MAPE (%)	R^2	Bias
ANN	0.124	0.353	0.220	4.5	0.958	-0.02
CNN	0.142	0.378	0.240	5.1	0.952	-0.05
LSTM	0.336	0.580	0.410	8.7	0.889	+0.12

Figure 5 illustrates a comparative analysis of error metrics across the three DL architectures. The ANN attained the smallest error values, with an MSE of 0.1246, an RMSE of 0.353, and a MAE of 0.220, in addition to the least MAPE of 4.5%. This indicates that ANN provided the most accurate and consistent predictions of reference evapotranspiration.

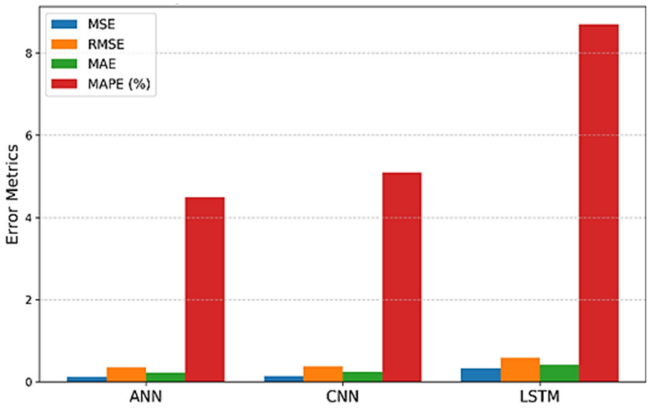

Fig. 5. Comparison of error metrics.

The CNN achieved performance comparable to the ANN, with slightly higher errors (MSE = 0.1426, RMSE = 0.378, MAE = 0.240, MAPE = 5.1%). It successfully captured some hierarchical relationships among variables despite the lack of explicit spatial structure in the data. In contrast, the LSTM model showed noticeably higher errors (MSE = 0.3361, RMSE = 0.580, MAE = 0.410, MAPE = 8.7%). Its weaker results stem from the dataset's static nature, which lacks the temporal dependencies required for sequential learning. Consequently, LSTM's complexity was underutilized, leading to poorer generalization.

TABLE III. COMPARISON OF MODELS

Model	R^2	Interpretation
ANN	0.958	Strong predictive accuracy, explains ~96% of variance
CNN	0.952	Nearly equal to ANN, robust prediction
LSTM	0.889	Lower accuracy, weaker variance explanation

TABLE IV. BIAS ANALYSIS OF MODELS

Model	Bias value	Interpretation
ANN	-0.02	Slight underprediction
CNN	-0.05	Noticeable underprediction
LSTM	+0.12	Overprediction tendency

TABLE V. MULTI-METRIC NORMALIZED PERFORMANCE

Model	MSE (scaled)	RMSE (scaled)	MAE (scaled)	MAPE (scaled)	R^2 (scaled)
ANN	0.63	0.61	0.61	0.65	1.00
CNN	0.58	0.56	0.56	0.58	0.99
LSTM	0.00	0.00	0.00	0.00	0.93

As shown in Table III, both ANN and CNN achieved high coefficients of determination ($R^2 \approx 0.95$), indicating that they explained nearly all variance in the observed ET_0 values. In contrast, the LSTM model performed weaker with an R^2 of 0.889. The bias analysis in Table IV shows that ANN (−0.02) and CNN (−0.05) slightly underestimate ET_0, while LSTM (+0.12) tends to overestimate. The normalized multi-metric evaluation in Table V supports these findings. The ANN consistently outperformed the other models across all error metrics, with CNN remaining close in performance and LSTM ranking lower. Overall, ANN demonstrated the most reliable and balanced results, CNN maintained competitive accuracy, and LSTM proved less effective due to its dependence on sequential data structures.

IV. CONCLUSION

Among the DL architectures evaluated, the ANN achieved the most balanced and accurate performance ($R^2 = 0.9588$, MSE = 0.1246) for ET_0 prediction at the Dharwad weather station. Its fully connected structure effectively captured nonlinear interactions among meteorological variables, making it well-suited for datasets without explicit spatial or temporal patterns. In contrast, the CNN ($R^2 = 0.9529$, MSE = 0.1426) showed comparable performance, while the LSTM model underperformed due to the absence of sequential dependencies. The key novelty of this study lies in demonstrating that when reference evapotranspiration datasets lack explicit spatial or temporal dependencies, simpler feed-forward architectures, such as ANN, outperform more complex models such as CNN and LSTM. This finding underscores that model selection must be data-driven, aligning architectural complexity with dataset characteristics—a critical but often overlooked aspect in ET_0 modeling. The study provides practical insight into how data topology influences DL performance in irrigation decision-support systems. These findings highlight that model selection should be driven by the intrinsic characteristics of the dataset rather than architectural complexity. For static meteorological input, ANN-based approaches offer a reliable, interpretable, and computationally efficient framework for irrigation decision-support systems. Future research will focus on integrating multi-source remote-sensing variables, including Normalized Difference Vegetation Index (NDVI) and Land-Surface Temperature (LST) from Sentinel-2 and MODIS, to capture spatio-temporal dynamics in ET_0 estimation.

ACKNOWLEDGMENT

The authors gratefully acknowledge the University of Agricultural Sciences, Dharwad, for providing the dataset. The support of the Department Chair, fellow research scholars, and the encouragement of family and friends have been instrumental in completing this study.

REFERENCES

[1] M. K. Gökkuş, "FAnfis Based Reference Evapotranspiration (ET0) Estimation Using Limited and Different Climate Parameters," *ISPEC Journal of Agricultural Sciences*, vol. 8, no. 4, pp. 1022–1033, Dec. 2024, https://doi.org/10.5281/ZENODO.13761632.

[2] H. D. Abeysiriwardana, N. Muttil, and U. Rathnayake, "A Comparative Study of Potential Evapotranspiration Estimation by Three Methods with FAO Penman–Monteith Method across Sri Lanka," *Hydrology*, vol. 9, no. 11, Nov. 2022, Art. no. 206, https://doi.org/10.3390/hydrology9110206.

[3] J. Rajput *et al.*, "Data-driven reference evapotranspiration (ET0) estimation: a comparative study of regression and machine learning techniques," *Environment, Development and Sustainability*, vol. 26, no. 5, pp. 12679–12706, Oct. 2023, https://doi.org/10.1007/s10668-023-03978-4.

[4] T. Wang *et al.*, "Hybrid Machine Learning Approach for Evapotranspiration Estimation of Fruit Tree in Agricultural Cyber–Physical Systems," *IEEE Transactions on Cybernetics*, vol. 53, no. 9, pp. 5677–5691, Sept. 2023, https://doi.org/10.1109/TCYB.2022.3164542.

[5] F. Alaieri, "Precision Agriculture based on Machine Learning and Remote Sensing Techniques," *Engineering, Technology & Applied Science Research*, vol. 14, no. 3, pp. 14206–14211, June 2024, https://doi.org/10.48084/etasr.6986.

[6] H. Salahudin *et al.*, "Using Ensembles of Machine Learning Techniques to Predict Reference Evapotranspiration (ET0) Using Limited Meteorological Data," *Hydrology*, vol. 10, no. 8, Aug. 2023, Art. no. 169, https://doi.org/10.3390/hydrology10080169.

[7] Y. Chang, C. Zhang, J. Huang, H. Chang, C. Wang, and Z. Huo, "Machine Learning for Reference Crop Evapotranspiration Modeling: A State-of-the-Art Review and Future Directions," *Agronomy*, vol. 15, no. 9, Aug. 2025, Art. no. 2038, https://doi.org/10.3390/agronomy15092038.

[8] X. Yan *et al.*, "Deep learning for daily potential evapotranspiration using a HS-LSTM approach," *Atmospheric Research*, vol. 292, Sept. 2023, Art. no. 106856, https://doi.org/10.1016/j.atmosres.2023.106856.

[9] Y. Rong *et al.*, "A Novel Hybrid Deep Learning Framework for Evaluating Field Evapotranspiration Considering the Impact of Soil Salinity," *Water Resources Research*, vol. 60, no. 9, Sept. 2024, Art. no. e2023WR036809, https://doi.org/10.1029/2023WR036809.

[10] S. Paul, S. Z. Farzana, S. Das, P. Das, and A. Kashem, "Comparative analysis of advanced deep learning models for predicting evapotranspiration based on meteorological data in Bangladesh," *Environmental Science and Pollution Research*, vol. 31, no. 50, pp. 60041–60064, Oct. 2024, https://doi.org/10.1007/s11356-024-35182-w.

[11] Y. Liu, S. Zhang, J. Zhang, L. Tang, and Y. Bai, "Assessment and Comparison of Six Machine Learning Models in Estimating Evapotranspiration over Croplands Using Remote Sensing and Meteorological Factors," *Remote Sensing*, vol. 13, no. 19, Sept. 2021, Art. no. 3838, https://doi.org/10.3390/rs13193838.

[12] A. A. Farooque *et al.*, "Forecasting daily evapotranspiration using artificial neural networks for sustainable irrigation scheduling," *Irrigation Science*, vol. 40, no. 1, pp. 55–69, Jan. 2022, https://doi.org/10.1007/s00271-021-00751-1.

[13] K. Irshad, N. Islam, A. A. Gari, S. Algarni, T. Alqahtani, and B. Imteyaz, "Arithmetic optimization with hybrid deep learning algorithm based solar radiation prediction model," *Sustainable Energy Technologies and Assessments*, vol. 57, June 2023, Art. no. 103165, https://doi.org/10.1016/j.seta.2023.103165.

[14] S. S. Sarkar, J. Bedi, and S. Jain, "A deep learning based framework for enhanced reference evapotranspiration estimation: evaluating accuracy and forecasting strategies," *Scientific Reports*, vol. 15, no. 1, Apr. 2025, Art. no. 15136, https://doi.org/10.1038/s41598-025-99713-2.

[15] S. Acharki *et al.*, "Comparative assessment of empirical and hybrid machine learning models for estimating daily reference evapotranspiration in sub-humid and semi-arid climates," *Scientific Reports*, vol. 15, no. 1, Jan. 2025, Art. no. 2542, https://doi.org/10.1038/s41598-024-83859-6.

[16] D. B. Upadhyaya *et al.*, "The Indian COSMOS Network (ICON): Validating L-Band Remote Sensing and Modelled Soil Moisture Data Products," *Remote Sensing*, vol. 13, no. 3, Feb. 2021, Art. no. 537, https://doi.org/10.3390/rs13030537.

[17] Y. Zhang, W. Han, H. Zhang, X. Niu, and G. Shao, "Evaluating maize evapotranspiration using high-resolution UAV-based imagery and FAO-56 dual crop coefficient approach," *Agricultural Water Management*, vol. 275, Jan. 2023, Art. no. 108004, https://doi.org/10.1016/j.agwat.2022.108004.

[18] N. G. Cutting, S. Kaur, M. C. Singh, N. Sharma, and A. Mishra, "Estimating Crop Evapotranspiration in Data-Scare Regions: A Comparative Analysis of Eddy Covariance, Empirical and Remote-Sensing Approaches," *Water Conservation Science and Engineering*, vol. 9, no. 2, Dec. 2024, Art. no. 65, https://doi.org/10.1007/s41101-024-00299-z.

[19] L. Xing *et al.*, "Estimating reference evapotranspiration using Penman-Monteith equation integrated with optimized solar radiation models," *Journal of Hydrology*, vol. 620, May 2023, Art. no. 129407, https://doi.org/10.1016/j.jhydrol.2023.129407.

[20] P. Aghelpour and R. Norooz-Valashedi, "Predicting daily reference evapotranspiration rates in a humid region, comparison of seven various data-based predictor models," *Stochastic Environmental Research and Risk Assessment*, vol. 36, no. 12, pp. 4133–4155, Dec. 2022, https://doi.org/10.1007/s00477-022-02249-4.

[21] B. Keshtegar, S. S. Abdullah, Y. F. Huang, M. K. Saggi, K. M. Khedher, and Z. M. Yaseen, "Reference evapotranspiration prediction using high-order response surface method," *Theoretical and Applied Climatology*, vol. 148, no. 1–2, pp. 849–867, Apr. 2022, https://doi.org/10.1007/s00704-022-03954-4.

[22] M. S. Aly, S. M. Darwish, and A. A. Aly, "High performance machine learning approach for reference evapotranspiration estimation," *Stochastic Environmental Research and Risk Assessment*, vol. 38, no. 2, pp. 689–713, Feb. 2024, https://doi.org/10.1007/s00477-023-02594-y.